

## Squeezing in an injection-locked semiconductor laser

S. Inoue,\* S. Machida, and Y. Yamamoto

*NTT Basic Research Laboratories, Musashino-shi, Tokyo 180, Japan*

H. Ohzu

*Department of Applied Physics, Waseda University, Shinjuku-ku, Tokyo 169, Japan*

(Received 26 October 1992)

The intensity-noise properties of an injection-locked semiconductor laser were studied experimentally. The constant-current-driven semiconductor laser producing the amplitude-squeezed state whose intensity noise was reduced below the standard quantum limit (SQL) by 0.72 dB was injection-locked by an external master laser. The measured intensity-noise level of the injection-locked semiconductor laser was 0.91 dB below the SQL. This experimental result indicates that a phase-coherent amplitude-squeezed state or squeezed vacuum state together with a reference local oscillator wave can be generated directly by semiconductor laser systems.

PACS number(s): 42.55.Px, 42.50.Dv

### I. INTRODUCTION

One of the most important applications of squeezed states is the improvement of an optical interferometer performance beyond the standard quantum limit, such as a gravitational-wave-detection interferometer. Direct generation of amplitude-squeezed states from a constant-current-driven semiconductor laser is the simplest and also so far one of the most efficient methods of generating squeezed states. The intensity noise reduced below the standard quantum limit (SQL) by more than 10 dB has been demonstrated [1]. However, this amplitude-squeezed state cannot be directly applied to improve an interferometric phase measurement. For this purpose, we need a phase-squeezed state or squeezed vacuum state together with a reference local oscillator. This has been

usually realized by a parametric down-conversion device. Recently the semiconductor-laser system that transforms amplitude-squeezed states into squeezed vacuum states has been proposed [2]. The key part in this system is amplitude-squeezed-state generation from an injection-locked semiconductor laser. In this paper we will show that the amplitude-squeezed state is indeed generated by an injection-locked semiconductor laser.

### II. THEORETICAL ANALYSIS

#### A. Quantum-mechanical Langevin equations for an injection-locked semiconductor laser

The Langevin equation for the cavity internal field  $\hat{A}(t)$  is given by [3]

$$\frac{d\hat{A}(t)}{dt} = -\frac{1}{2} \left[ \frac{\omega}{Q} + i2(\omega_r - \omega) - \frac{\omega}{\mu^2} (\tilde{\chi}_i - i\tilde{\chi}_r) \right] \hat{A}(t) + \left[ \frac{\omega}{\mu^2} \langle \tilde{\chi}_i \rangle \right]^{1/2} \hat{f}_G(t) + \left[ \frac{\omega}{Q_0} \right]^{1/2} \hat{f}_L(t) + \left[ \frac{\omega}{Q_e} \right]^{1/2} [F_0 + \hat{f}(t)], \tag{2.1}$$

where  $F_0$  is the classical (*c*-number) excitation of the injection signal and  $\hat{f}(t)$  is the injection-signal fluctuation operator. The noise operators  $\hat{f}_G(t)$  and  $\hat{f}_L(t)$  are associated with the gain fluctuation and the internal loss, respectively. The optical angular frequency of the injection signal and the angular resonance frequency of the unpumped cavity is denoted by  $\omega$  and  $\omega_r$ . The total  $Q$  value of the laser cavity depends on the external (mirror) loss  $Q_e$  and the internal loss  $Q_0$  according to

$$\frac{1}{Q} = \frac{1}{Q_e} + \frac{1}{Q_0}. \tag{2.2}$$

$\mu$  is the refractive index and  $\tilde{\chi}$  is the electronic susceptibility operator, whose imaginary part equals the stimulat-

ed emission gain:

$$\frac{\omega}{\mu^2} \tilde{\chi}_i = \tilde{E}_{cv} - \tilde{E}_{vc}, \tag{2.3}$$

where  $\tilde{E}_{cv}$  and  $\tilde{E}_{vc}$  are the operators of the stimulated emission and absorption rates. The linewidth enhancement factor  $\alpha$  is defined by

$$\alpha = \frac{d\langle \tilde{\chi}_r \rangle}{dN_{c0}} / \frac{d\langle \tilde{\chi}_i \rangle}{dN_{c0}}, \tag{2.4}$$

where  $N_{c0}$  is the average excited electron number.

The Langevin equation for the total excited-electron-number operator  $\hat{N}_c(t)$  is given by

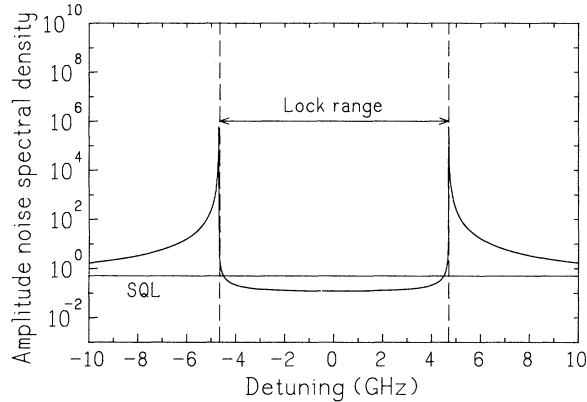
$$\frac{d\tilde{N}_c(t)}{dt} = p - \frac{\tilde{N}_c(t)}{\tau_{sp}} - (\tilde{E}_{cv} - \tilde{E}_{vc})\hat{n}(t) - \langle \tilde{E}_{cv} \rangle + \tilde{\Gamma}_p(t) + \tilde{\Gamma}_{sp}(t) + \tilde{\Gamma}(t), \quad (2.5)$$

where  $p$  is the pumping rate,  $\tau_{sp}$  is the lifetime of the electrons due to spontaneous emission and  $\hat{n}(t) \equiv \hat{A}^\dagger(t)\hat{A}(t)$  is the photon-number operator. The noise operators  $\tilde{\Gamma}_p(t)$ ,  $\tilde{\Gamma}_{sp}(t)$ , and  $\tilde{\Gamma}(t)$  are associated with the pump noise, the spontaneous emission noise, and the stimulated emission and absorption noise (including spontaneous emission into a lasing mode), respectively.

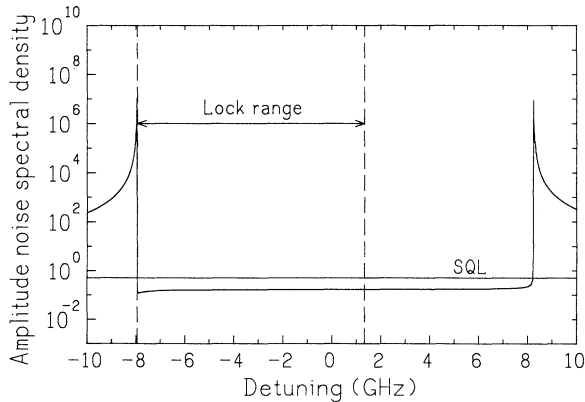
These two Langevin equations (2.1) and (2.5) are solved by the quasilinearization procedure described in Refs. [3],[4]. The cavity external photon field  $\hat{r}(t)$  is related to the cavity internal photon field  $\hat{A}(t)$  and the injection signal  $F_0 + \hat{f}(t)$  by the following equation:

$$\hat{r}(t) = -[F_0 + \hat{f}(t)] + \left[ \frac{\omega}{Q_e} \right]^{1/2} \hat{A}(t). \quad (2.6)$$

Finally the external amplitude-noise spectral density  $\langle \Delta\hat{r}(\Omega)\Delta\hat{r}(\Omega) \rangle$  is calculated by using the correlation functions between the noise operators.



(a)



(b)

FIG. 1. The external amplitude-noise spectral density at  $\Omega=0$  as a function of the detuning (a)  $\alpha=0$ , (b)  $\alpha=6$ .

## B. Numerical results

The external amplitude-noise spectral densities at  $\Omega=0$  are calculated numerically as a function of the detuning, which is defined by the difference between the frequency of the injection signal and the resonance frequency of the cavity. The following numerical parameters are assumed for the diode laser:  $\tau_{sp}=2 \times 10^{-9}$  s,  $\tau_p=2 \times 10^{-12}$  s,  $\tau_{pe}=2.5 \times 10^{-12}$  s,  $\beta=2 \times 10^{-5}$ , and  $n_{sp}=1$ , where  $\tau_p$  and  $\tau_{pe}$  are photon lifetimes corresponding to  $Q$  and  $Q_e$ ,  $\beta$  is the spontaneous-emission coefficient and  $n_{sp}$  is the population inversion factor. The pump rate  $R(\equiv I/I_{th}-1)=10$ . The values of  $F_0$  are  $4.8 \times 10^7$  in the case of  $\alpha=0$  and  $1.34 \times 10^7$  in the case of  $\alpha=6$ . In both cases, the locking bandwidth is 9.3 GHz. The pump noise is completely suppressed, that is,  $\langle \tilde{\Gamma}_p^\dagger(t)\tilde{\Gamma}_p(u) \rangle = 0$ .

Figures 1(a) and 1(b) show the external amplitude-noise spectral densities as a function of the detuning with the linewidth enhancement factor  $\alpha=0$  and  $\alpha=6$ , respectively. These numerical results are valid within the locking bandwidth because it is assumed in Eq. (2.1) that the angular frequency of the injection signal is identical to the resonance frequency of the cavity. In the case of  $\alpha=0$  [Fig. 1(a)], the amplitude noise spectral density, and locking bandwidth are symmetric and the minimum noise value is seen at the detuning  $\Delta f=0$ . In this case, the amplitude squeezing is seen only within the locking bandwidth. In the case of  $\alpha=6$  [Fig. 1(b)], the amplitude-noise spectral density and the locking bandwidth are asymmetric, and the minimum value of the amplitude noise is seen close to the negative edge of the locking bandwidth.

## III. EXPERIMENTAL SETUP

The experimental setup is shown in Fig. 2. The master laser is an Al-Ga-As single-mode high-power semiconductor laser. This master laser is mounted on a copper heat sink in a temperature-controlled chamber. Two optical isolators are used in tandem to avoid the undesired

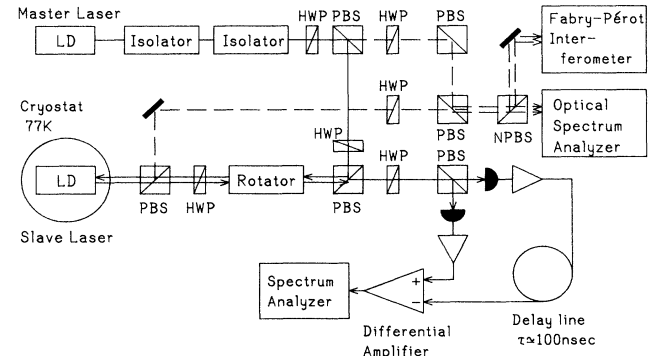


FIG. 2. The experimental setup for the measurement of the intensity noise of an injection-locked semiconductor laser. HWP, half-wave plate; PBS, polarization beam splitter; NPBS, nonpolarization beam splitter.

feedback from the slave laser. The slave laser is a single-mode low-power GaAs transverse-junction strip semiconductor laser with antireflection coating ( $\sim 10\%$ ) on the front facet and high-reflection coating ( $\sim 90\%$ ) on the rear facet. This slave laser is also mounted on a copper heat sink in a 77-K cryostat. Two polarization beam splitters, one half-wave plate and one Faraday rotator in front of the slave laser, are used to match the master-laser polarization to the slave-laser polarization and to avoid the undesired feedback from the detection system. The master- and slave-laser outputs are collimated with antireflection-coated microlenses. The oscillation wavelengths of the master and slave lasers are simultaneously monitored by an optical-spectrum analyzer and a Fabry-Pérot interferometers. Longitudinal mode matching between the two lasers is carried out roughly by controlling the temperature of the master-laser heat sink. The optical-spectrum analyzer is used to identify the longitudinal modes roughly. Frequency fine tuning is achieved by adjusting the master-laser drive current. The Fabry-Pérot interferometer is used to observe the locking phenomena.

The detection system is a balanced direct detector with a delay line [5]. In this detection system, two identical *p-i-n* photodiodes (HAMAMATSU S1721) are used and they are biased at 70 V. The signal wave is equally divided by a half-wave plate and a polarization beam splitter. One detector output is delayed by about 100 ns, but the other detector output is not. The difference in these two outputs is produced by a differential amplifier. For a fluctuation frequency  $\Omega_{in}$  satisfying the in-phase delay condition,  $\Omega_{in}\tau = 2N\pi$ , where  $\tau$  is a delay time and  $N$  is an integer, the differential amplifier output measures  $I_1 - I_2$ , where  $I_1$  and  $I_2$  are the two photodetector currents. Quantum-mechanical analysis of a balanced detector shows that  $I_1 - I_2$  corresponds to the quantum noise of a vacuum field at the signal channel with polarizations perpendicular to the signal field and that the current-fluctuation spectral density is exactly equal to the shot-noise level. For a fluctuation frequency  $\Omega_{out}$  satisfying the out-of-phase delay condition,  $\Omega_{out}\tau = (2N + 1)\pi$ , the differential-amplifier output measures  $I_1 + I_2$ . The quantum-mechanical theory of a balanced detector shows that  $I_1 + I_2$  corresponds to the quantum noise of the signal wave with polarizations parallel to the signal field. Thus the detector output simultaneously displays the signal-noise level and the corresponding shot-noise level on a spectrum analyzer with a frequency period of  $\Delta\Omega = 2\pi/\tau$ . In the calibration of the shot-noise level using another light source, there exists some ambiguity due to light-intensity fluctuations, changes in the signal beam position and photodetector saturation. However, this ambiguity is eliminated in our detection system, because the quantum noise of the signal field and that of a vacuum field are simultaneously measured under the same conditions. Furthermore there is no possibility that the enhanced squeezing measured is due to photodetector saturation.

To eliminate a minute optical-reflection feedback to the slave laser, all optical elements are antireflection coated and slanted with respect to the beam direction.

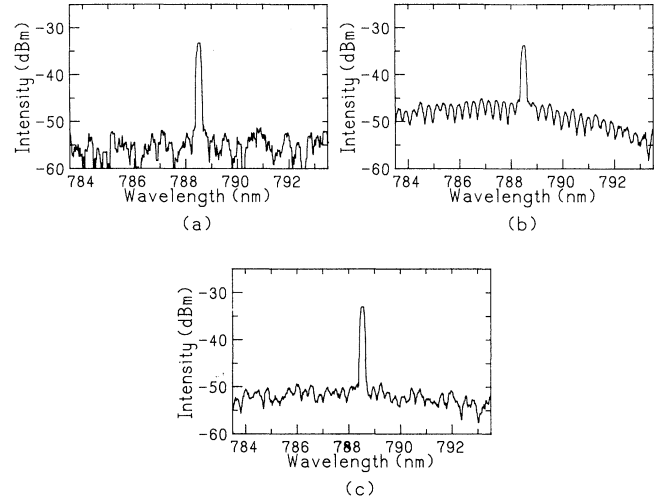


FIG. 3. The spectra of (a) master, (b) slave, (c) and injection-locked semiconductor lasers.

## IV. EXPERIMENTAL RESULTS

### A. Spectra of master, slave, and injection-locked lasers

Figures 3(a) and 3(b) show the spectra of master and slave lasers. The oscillation wavelength of the slave laser is 788.6 nm at 77 K and  $I_d = 18$  mA. The oscillation wavelength of the master laser is matched to the same wavelength. Figure 3(c) shows the spectrum of an injection-locked laser. It is demonstrated that the side-mode intensity of the slave laser is suppressed by about 5 dB due to injection locking.

### B. Observation of an injection-locking phenomena by a Fabry-Pérot interferometer

Figure 4(a) shows a Fabry-Pérot interferometer output without injection locking. The linewidths of the master and slave lasers are 75 and 72.5 MHz, respectively. Figure 4(b) shows a Fabry-Pérot interferometer output with injection locking. It is demonstrated that the oscillation frequency of the slave laser is locked to that of the master laser by injection-locking.

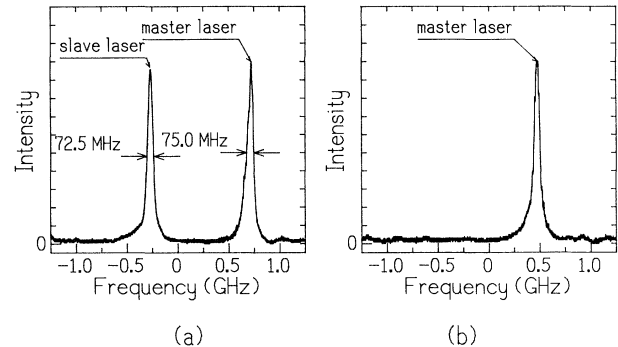


FIG. 4. Fabry-Pérot interferometer output (a) without injection locking and (b) with injection locking.

### C. Intensity-noise spectra for the free-running master and slave laser

Figure 5 shows the differential amplifier output spectra. Curves (a) and (b) show the intensity-noise spectra for the free-running master and slave lasers, respectively. These spectra are modulated at the frequency of 10 MHz because the output signal of one detector is delayed by 100 ns. Therefore, the laser intensity noise and the corresponding shot-noise value appear in the frequency of 10 MHz. The intensity-noise spectrum for the master laser, which is shown by curve (a), features lower noise power at  $\Omega_{in}$  than at  $\Omega_{out}$ . This indicates that the master-laser output field has excess amplitude noise. On the other hand, the intensity-noise spectrum for the slave laser, which is shown by curve (b), features higher noise power at  $\Omega_{in}$  than at  $\Omega_{out}$ . This indicates that the slave-laser output field has squeezed amplitude noise. The slave-laser drive current is 18 mA which corresponds to 13.3 times the threshold current. The total dc photocurrent for this bias level is 5.14 mA, which is not the same as that for the master laser. Curve (c) shows the output spectrum of a single detector, that is, one of the two signal beams is blocked. This curve shows the frequency characteristics of our detection system, which is used to correct the shot-noise value at  $\Omega_{out}$ . Curve (d) shows the thermal-noise value which is about 10 dB below the curve (c) in the low-frequency region.

### D. Intensity-noise spectral density of an injection-locked semiconductor laser

Figure 6 shows the intensity-noise spectral density of an injection-locked semiconductor laser at 23.9 MHz as a function of the master-laser frequency detuning from the slave-laser free-running frequency. The intensity-noise spectral density is normalized by the corresponding shot-noise value. The slave laser drive current is 18 mA which corresponds to 13.3 times the threshold current.

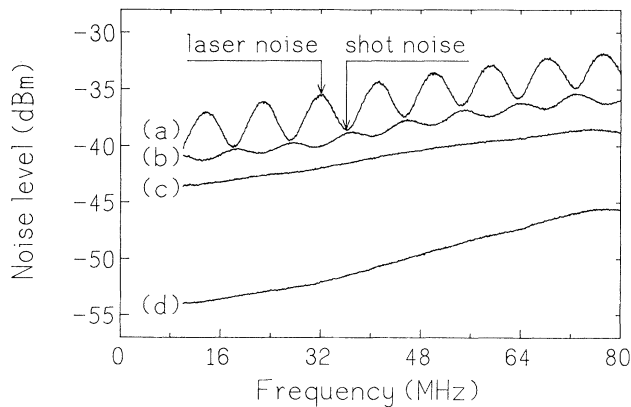


FIG. 5. Intensity-noise spectra for (a) the master laser, (b) the free-running slave laser, (c) the output of single detector, and (d) the thermal noise.

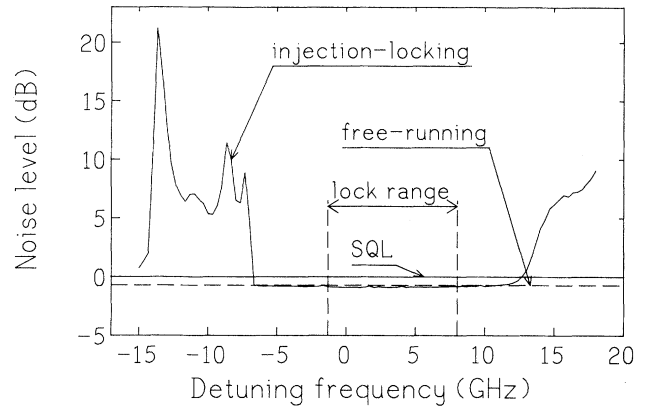


FIG. 6. Intensity-noise spectral density of an injection-locked semiconductor laser as a function of the detuning.

The total dc photocurrent without injection locking is 5.14 mA and that with injection locking is 5.06 mA. The slight decrease of the output power by injection locking is due to the cavity internal loss [3]. The dashed line shows the intensity-noise spectral density of a free-running slave laser, which is 0.72 dB below the standard quantum limit. The injection power into the slave laser, which is measured in front of the cryostat, is 7 mW. The locking bandwidth is measured to be 9.3 GHz. The minimum value of the measured noise level of the injection-locked semiconductor laser is 0.91 dB below the SQL. This corresponds to  $-2.56$  dB squeezing when corrected for an optical loss from the laser to the detector. The linewidth enhancement factor  $\alpha$  is estimated to be about 6 from the asymmetry of the locking bandwidth.

Comparing this experimental result with the numerical results presented in Sec. II [Fig. 1(b)] and in Ref. [3], we can find the following different points. In the experimental result, amplitude squeezing was enhanced by injection locking although it is not enhanced but rather degraded in the numerical result. This enhancement of amplitude squeezing is due to the suppression of the side-mode intensity of the slave laser by injection locking [Fig. 3(c)], because the suppression of the side-mode intensity reduces the mode-partition noise caused by the multi-longitudinal-mode oscillation [6]. Even in the case that the free-running slave laser is in a multi-longitudinal-mode oscillation and its intensity noise is excess noise, we observed the squeezed intensity noise by suppressing the side-mode intensity in terms of injection locking. In order to explain the above-mentioned phenomenon, we must analyze the injection locking to the slave laser which is not in a single-mode oscillation but in a multi-longitudinal-mode oscillation. Amplitude squeezing is observed even outside of the negative edge of the locking bandwidth. Outside of the locking bandwidth where amplitude squeezing was observed, the slave-laser frequency changes with a constant frequency separation to the master-laser frequency. The asymmetry of the locking bandwidth in the experimental result is opposite to that of the numerical result. These points require further theoretical study.

## V. CONCLUSION

The squeezed intensity fluctuation was observed in an injection-locked semiconductor laser. The phase coherence between the injection-locked slave-laser output and the master-laser output was also confirmed by observing the interference fringe. This paper demonstrates that the amplitude-squeezed state is not destroyed but rather enhanced by injection locking. This amplitude-squeezed state from the slave laser is phase coherent with the

master-laser output, so there will be numerous application for such a phase-coherent amplitude-squeezed state. One of them is the FM noise spectroscopy with a squeezed probe wave and a high-intensity pump (saturating) wave. It is also possible to cancel the coherent excitation of the squeezed output signal from the injection-locked slave laser by destructive interference with the master-laser signal without degrading the squeezing by using a high-transmission mirror, and a squeezed vacuum state will be generated.

---

\*Permanent address: Department of Applied Physics,  
Waseda University, Shinjuku-ku, Tokyo 169, Japan.

- [1] W. H. Richardson, S. Machida, and Y. Yamamoto, *Phys. Rev. Lett.* **66**, 2867 (1991).
- [2] Y. Lai, H. A. Haus, and Y. Yamamoto, *Opt. Lett.* **16**, 1517 (1991).
- [3] L. Gillner, G. Björk, and Y. Yamamoto, *Phys. Rev. A* **41**,

5053 (1990).

- [4] H. A. Haus and Y. Yamamoto, *Phys. Rev. A* **29**, 1261 (1984).
- [5] S. Machida and Y. Yamamoto, *Opt. Lett.* **14**, 1045 (1989).
- [6] S. Inoue, H. Ohzu, S. Machida, and Y. Yamamoto, *Phys. Rev. A* **46**, 2757 (1992).